



# 1 The influence of human activities on streamflow reductions during the 2 megadrought in Central Chile

3 Nicolás Álamos<sup>1,2,3</sup>, Camila Alvarez-Garreton<sup>1</sup>, Ariel Muñoz<sup>1,3,4</sup>, Álvaro González-Reyes<sup>2,5,6,7</sup>

4 <sup>1</sup>Center for Climate and Resilience Research (CR2, FONDAP 1522A0001), Santiago, Chile

5 <sup>2</sup>Instituto de Ciencias de la Tierra ICT, Facultad de Ciencias, Universidad Austral de Chile

6 <sup>3</sup>Centro de Acción Climática, Pontificia Universidad Católica de Valparaíso

7 <sup>4</sup>Laboratorio de Dendrocronología y Estudios Ambientales, Instituto de Geografía, Pontificia Universidad Católica de  
8 Valparaíso, Chile

9 <sup>5</sup>Centro de Humedales río Cruces CEHUM, Universidad Austral de Chile, Chile

10 <sup>6</sup>Laboratorio de Dendrocronología y Cambio Global, Universidad Austral de Chile, Valdivia, Chile

11 <sup>7</sup>Centro de Investigación: Dinámica de Ecosistemas Marinos de Altas Latitudes - IDEAL, Chile

12 *Correspondence to:* Camila Alvarez Garreton ([calvarezgarreton@gmail.com](mailto:calvarezgarreton@gmail.com))

13 **Abstract.** Central Chile has experienced a protracted megadrought since 2010 (up to date), with annual precipitation deficits  
14 ranging from 25% to 70%. Drought propagation has been intensified during this time, with streamflow reductions up to 30%  
15 larger than those expected from historical records. This intensification has been attributed to the cumulative effect of  
16 precipitation deficits associated to catchment memory in near-natural basins of central Chile. However, the additional effect  
17 of water extractions on drought intensification in disturbed basins remains an open challenge. In this study, we assess the  
18 effects of climate and water use on streamflow reductions during the last three decades in four major agricultural basins in  
19 central Chile, with particular focus on the ongoing megadrought. We address this by contrasting streamflow observations with  
20 near-natural streamflow simulations representing the discharge that would have occurred without water extractions. Near-  
21 natural streamflow estimations are obtained from rainfall-runoff models trained over a reference period with low human  
22 intervention (1960-1988). We characterise hydrological droughts driven by precipitation and human activities during the  
23 evaluation period (1988-2020) in terms of the frequency, duration and intensity of near-natural and observed seasonal  
24 streamflow deficits, respectively.

25 Our results show that before the megadrought onset (1988-2009), streamflow in the four basins was 2 to 20% lower than the  
26 streamflow during the undisturbed period. Between 81 to 100% of these larger deficits were explained by water extractions.  
27 During the megadrought (2010-2020), streamflow was reduced in a range of 47 to 76 % among the different basins, compared  
28 to the reference period. During this time, the climatic contribution to streamflow reductions increased and water extractions  
29 had a lower relative contribution, accounting for 27 to 51% of streamflow reduction. During the complete evaluation period,  
30 human activities have amplified the propagation of droughts, with more than double the frequency, duration, and intensity of  
31 hydrological droughts in some basins, compared to those expected by precipitation deficits only. We conclude that while the  
32 primary cause of streamflow reductions during the megadrought has been the lack of precipitation, water uses have not



33 diminished during this time, causing an exacerbation of the hydrological drought conditions and aggravating their impacts on  
34 human water consumption, economic activities, and natural ecosystems.

## 35 **1 Introduction**

36 The fluxes of the water cycle vary and change in time and space, as well as the anthropic activities affecting those fluxes,  
37 leading to a co-evolving hydrosocial cycle (Linton and Budds, 2014; Budds, 2012) that defines the state of the hydrological  
38 system (Van Loon et al., 2016). Observational evidence in different regions indicates that hydrological cycles are being  
39 affected by climate change and human activities. Climate change has led to changes in precipitation patterns worldwide (Fleig  
40 et al., 2010; Kingston et al., 2015), while human activities have altered the spatiotemporal distribution of water resources (Van  
41 Loon et al., 2022). This can potentially generate water scarcity problems, particularly when precipitation deficits occur in  
42 regions that concentrate water consumption requirements.

43 While meteorological droughts (precipitation deficits) are mainly controlled by regional climate, hydrological droughts  
44 (streamflow, and groundwater deficits) are also influenced by catchment characteristics and water uses. In this way, under  
45 similar meteorological conditions, the severity of hydrological droughts and their impacts on society can vary significantly  
46 within the territory (Van Lanen et al., 2013).

47 Most drought analyses consider climate variability as a main driver of drought, however, increasing focus has been given to  
48 assessing the compounding effects of climate variability and human activities on water resources and drought propagation  
49 (Van Loon et al., 2016; Wanders and Wada, 2015; Zhao et al., 2014). Anthropogenic activities, such as irrigation, urbanization,  
50 land use changes, and water infrastructure (e.g., reservoirs or water transfer channels) affect runoff mechanisms (Huang et al.,  
51 2016) and can lead to a higher frequency of hydrological droughts (Alvarez-Garreton et al., 2021; Ward et al., 2020). A notable  
52 example of this is the Yellow river basin in China, where despite not significant rainfall deficits have occurred in recent years,  
53 a hydrological drought with historical minimum flow levels is being observed, which has been mainly dominated by anthropic  
54 uses in the basin (Huang et al., 2016; Kong et al., 2016; Li et al., 2019; Liu et al., 2016; Zhao et al., 2014).

55 Advancing our understanding of hydrological droughts as a complex process depending on the interaction between climatic,  
56 biophysical, and anthropic drivers is critical to assess a catchment's vulnerability to droughts, mitigate their occurrence, and  
57 design adaptation plans. While all these drivers influence the propagation and impacts of droughts, adaptation and mitigation  
58 water management plans mainly influence on human activities. Therefore, it is critical to address the scientific challenge of  
59 understanding the influence of human activities on the hydrological cycle and quantifying their impacts.



60 To address this challenge, in this paper we focus in central Chile (29°-35°S; Fig. 1), a region where the signal of anthropogenic  
61 climate change is leading to an increase in mean temperature, increasing of heatwaves events, and a sustained decrease in  
62 precipitation (Boisier et al., 2018; Bozkurt et al., 2017; Garreaud et al., 2017, 2020; González-Reyes et al., 2023). The drying  
63 trend has led to the so-called megadrought, affecting the country since 2010, with annual precipitation deficits ranging between  
64 25% and 70% (Garreaud et al., 2020, 2017). This meteorological drought in central Chile has propagated across the terrestrial  
65 system, leading to hydrological droughts and water scarcity problems that vary across the territory (Alvarez-Garreton et al.,  
66 2021; Duran-Llacer et al., 2020; Muñoz et al., 2020; Barría et al., 2021b).

67 For example, in the Petorca river basin, Muñoz et al. (2020) found that during the megadrought, streamflow, and water bodies  
68 of the upper parts of the basin were less affected than the mid and low areas of the valley, where most of the agriculture is  
69 located. However, the authors did not make a formal attribution study to disentangle the role of water consumption and climate  
70 on streamflow reduction. Another study was conducted on the Aculeo Lake, a natural reservoir in central Chile that dried up  
71 during the ongoing megadrought. Barría et al (2021b) performed an attribution exercise and used the Water Evaluation and  
72 Planning System (WEAP) hydrological model and concluded that climate was the primary factor explaining the lake's drying,  
73 while water demand has remained stable over the past few decades. Furthermore, higher than expected streamflow reductions  
74 during the megadrought have also been observed in near-natural basins. Alvarez-Garreton et al. (2021) reported the effects of  
75 catchment memory in snow-dominated catchments in Central Chile, where the accumulation of the persistent precipitation  
76 deficits led to less streamflow than expected from observations during previous single-year meteorological droughts. Although  
77 there have been some insights of the role of catchments and anthropic characteristics in the megadrought's propagation, the  
78 impact of human activities on streamflow reduction and drought conditions in the major basins of central Chile remains unclear.

79 In this article, we quantify the relative effects of climate and water extractions on streamflow reduction during the megadrought  
80 (2010-2020) and before it (1988-2010) in four major agricultural basins in central Chile. Additionally, we assess the influence  
81 of water extractions on the intensity, frequency, and duration of hydrological droughts for the same period. To achieve this,  
82 we follow the approach proposed by Van Loon et al. (2022) and compare streamflow observations with a near natural simulated  
83 flow representing the discharge that would have occurred without human influences.

## 84 **2 Methods and data**

### 85 **2.1 Study area**

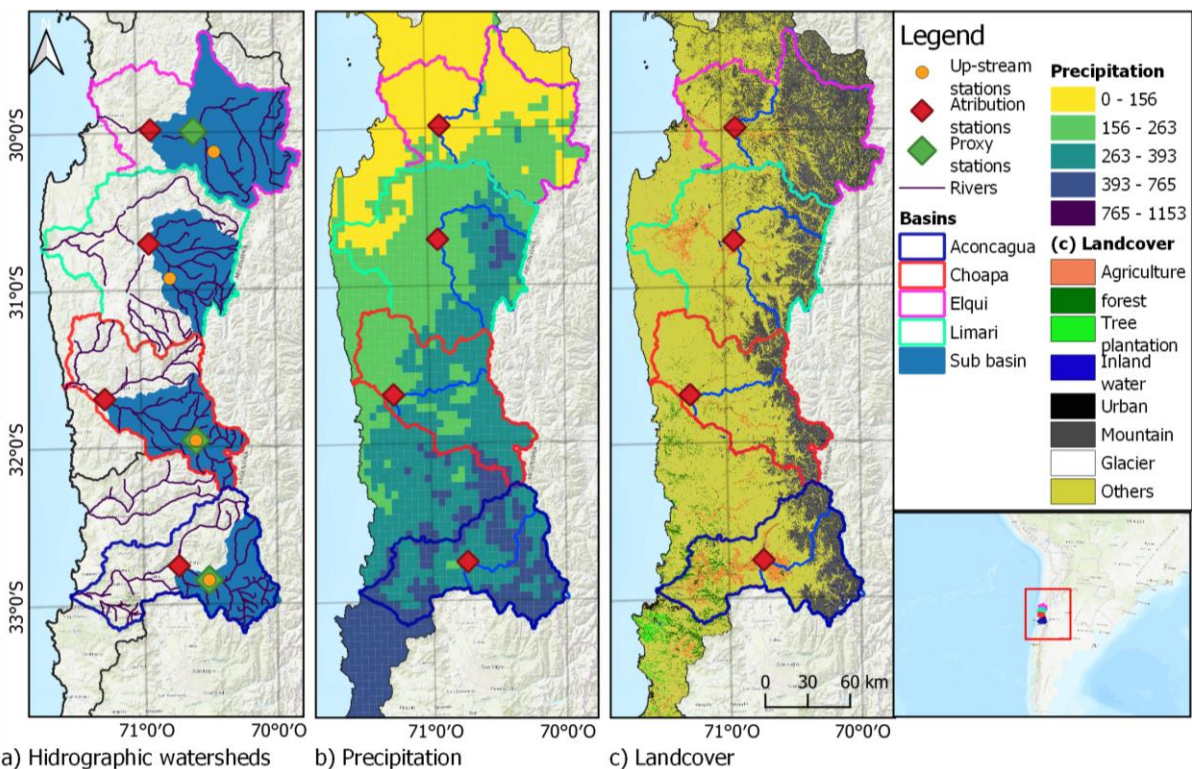
86 The study was conducted in four major basins located between 29° and 33°S (Fig. 1): The Elqui, Limarí, and Choapa basins  
87 in the Coquimbo region, and the Aconcagua basin in the Valparaíso region. These basins fall within semi-arid (Coquimbo



88 region) and mediterranean (Valparaiso region) climate zones, which are particularly vulnerable to droughts due to the majority  
89 of annual precipitation occurring during a few winter events (Garreaud et al., 2017).

90 All catchments feature a snow-rain-fed hydrologic regime. The Aconcagua basin also has a large glacier area (192 km<sup>2</sup>) that  
91 contributes to runoff, especially during dry summers (Crespo et al., 2020). The study basins have experienced precipitation  
92 deficits of 25-70% and streamflow deficits of up to 70% during the megadrought that has affected the region since 2010  
93 (Alvarez-Garretton et al., 2021; Garreaud et al., 2020, 2017).

94 According to the data provided by the water security platform from the Center for Climate and Resilience Research  
95 ([www.seguridadhidrica.cl](http://www.seguridadhidrica.cl)), agriculture is the primary productive sector and the main consumer of water resources within these  
96 basins. Agricultural lands cover areas of 152 km<sup>2</sup>, 605 km<sup>2</sup>, 313 km<sup>2</sup>, and 582 km<sup>2</sup>, and their annual water consumption at  
97 present corresponds to 3.25 m<sup>3</sup>/s, 14.3 m<sup>3</sup>/s, 6.48 m<sup>3</sup>/s, and 15.72 m<sup>3</sup>/s, in the Elqui, Limarí, Choapa, and Aconcagua basins,  
98 respectively. Avocado and table vine species are the main consumers in the Aconcagua basin, while the Limarí basin has a  
99 higher demand from permanent forage species, table vine, and citrus plantations.



100

101 **Figure 1.** Panel a) shows the four main basins of the study area and the streamflow gauges used for the analyses. The red diamonds  
 102 indicate the stations used to characterise each basin; the green diamonds are the gauges used as predictors for filling in monthly  
 103 streamflow data (Sect. 2.2); and the orange circles are the up-stream stations used in the rainfall-runoff ratio analysis (Sect. 2.3).  
 104 The basin area covered by the red diamond gauge is painted blue. Panel b) presents the mean annual precipitation (mm/yr) from  
 105 the CR2MET dataset for the period 1980-2010. Panel c) shows the gridded land cover dataset from Zhao et al. (2016). Base map  
 106 source: Esri, 2017.

107 **2.2 Data**

108 Times series of monthly streamflow and runoff (streamflow normalised by catchment area) were obtained from the CAMELS-  
 109 CL dataset (Alvarez-Garreton et al., 2018; available at: <https://camels.cr2.cl/>) for the period April 1960 – March 2020.  
 110 Catchment-scale monthly precipitation for the same period was obtained from the CR2MET dataset version 2.5 at a 5 x 5 km  
 111 grid resolution (Boisier, 2023) and averaged across the basin polygons. Catchment-scale monthly evapotranspiration (ET) was  
 112 computed based on the ECMWF surface re-analysis ERA5-Land dataset, available at a horizontal resolution of 10 km (Muñoz-  
 113 Sabater et al., 2021) from April 1960 to March 2020. For each study basin, we selected the most downstream streamflow gauge  
 114 station having more than 80% of streamflow records for the 1960-2020 period (see Fig. 1). Gaps in monthly streamflow of  
 115 downstream gauges (red diamonds in Fig. 1a) were filled based on linear regression models, using the basin's precipitation and  
 116 the streamflow of an upstream gauge with a strong correlation with the considered station (green diamonds in Fig. 1a) as



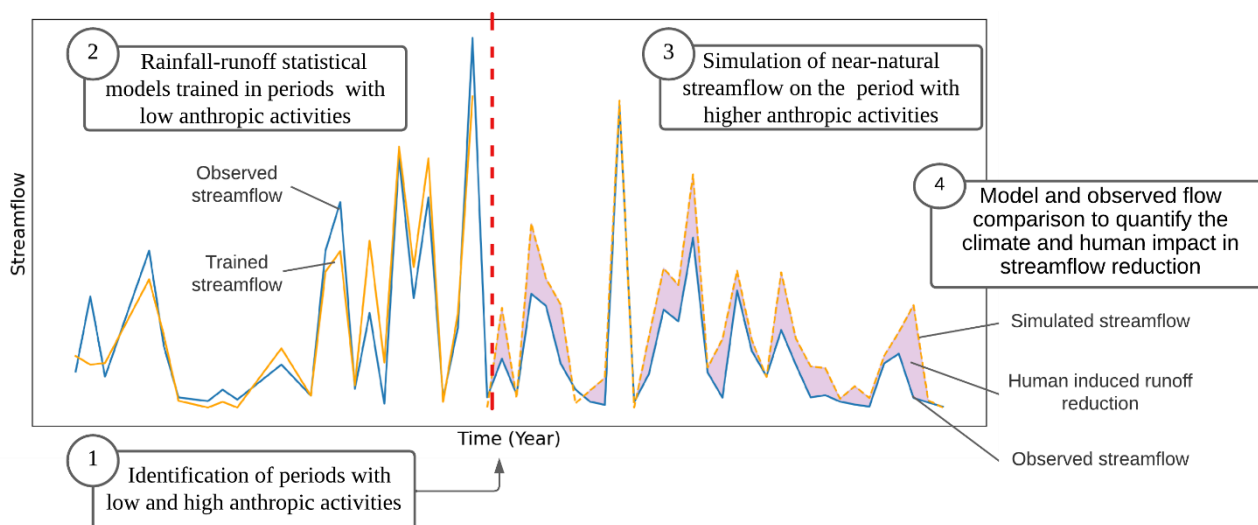
117 predictors. The linear regressions resulted in coefficients of determination larger than 0.8 in Elqui, Choapa, and Aconcagua  
118 basins.

119 Streamflow and basin-averaged precipitation and ET were computed for hydrological years (April to March in Chile) and for  
120 wet and dry seasons. The wet season is defined from April to August, while the dry season corresponds to the months between  
121 September and March. Annual (seasonal) streamflow values were computed when the 12 (6) months had valid data.

122 To account for human intervention within the basins, we analysed annual water uses from industry, energy, mining, livestock,  
123 drinking water sectors, as well as water evaporation from lakes and reservoirs for the period 1960-2020 obtained from the  
124 water security platform from the Center for Climate and Resilience Research ([www.seguridadhidrica.cl](http://www.seguridadhidrica.cl)). All variables with a  
125 different spatial resolution than the basin (whether gridded or associated with an administrative unit) were calculated for the  
126 basin considering the weighted average of the variable within the basin surface.

### 127 2.3 Near-natural streamflow modelling and attribution exercise

128 The attribution exercise to quantify the climatic and human contributions on streamflow reductions is schematized in Fig. 2.  
129 Near-natural streamflow simulations were obtained by rainfall-runoff statistical models trained in periods when anthropic  
130 activities had low water consumption (Sharifi et al., 2021; Zhao et al., 2014).



131

132 **Figure 2. Flowchart of the steps to quantify the human contribution to streamflow reduction based on comparing a near-natural**  
133 **simulated streamflow with the observed streamflow on a period of high anthropic activities.**



### 134 **2.3.1 Selection of low-influence training periods**

135 For each basin, we identified low human intervention periods based on the regime shifts of streamflow, precipitation, and  
136 anthropic variables (Sect. 2.2). The non-parametric Buishand break point test (Buishand, 1982) was applied to identify regime  
137 shifts. Buishand is a statistical homogeneity test method that checks if two (or more) datasets come from the same distribution.  
138 In this way, the test can detect breakpoints where the distribution of a dataset changes. We applied the Buishand test to each  
139 time series during the 1960-2020 periods. To identify multiple breakpoints, we iterated the test in the sub-periods before and  
140 after the previous breakpoint until no breakpoints with a significance level at p-value < 0.05. For the Buishand test, we used  
141 the pyHomogeneity Python library (Shourov, 2020).

142 Subsequently, a singular training period was selected across basins based on the identification of concurrent breaking points  
143 in both streamflow and human activities time series, while ensuring the absence of discernible precipitation shifts. By  
144 employing this approach, we ensure the selection of streamflow breakpoints that are not predominantly influenced by climatic  
145 variations.

146 To ensure that the chosen period of analysis is not dependent on the specific statistical test employed, we conducted a sensitivity  
147 analysis using the Sequential T-test Analysis of Regime Shifts (STARS) at a monthly time scale for both precipitation and  
148 streamflow time series (Rodionov, 2004). The STARS V6.3 Excel macro application, available at  
149 <https://sites.google.com/view/regime-shift-test> was utilized to perform the Rodionov test.

### 150 **2.3.2 Climate and human contribution to streamflow reduction**

151 Assuming that the effects of climate and local human activities on streamflow generation are independent, the observed  
152 streamflow ( $Q_{obs}$ ) can be disaggregated as follows (Kong et al., 2016):

$$153 \quad Q_{obs} = Q_{nn} + \Delta Q_{human} \quad (1)$$

154 Where  $Q_{nn}$  corresponds to a climatic-induced streamflow, referred as near-natural streamflow in this paper, and  $\Delta Q_{human}$  is  
155 the human-induced effect on streamflow. In this study, near-natural streamflow in Eq.1 is estimated from linear rainfall-runoff  
156 regressions trained in the low-influence reference period defined in Sect. 2.3.1. To account for pluvial and snowmelt runoff  
157 generation processes, we implemented seasonal rainfall-runoff models. In several snow-dominated basins in central Chile, the  
158 winter flows continue to be fed by the snow accumulation of the previous hydrological year, especially when the previous year  
159 was wetter than normal (Alvarez-Garreton et al., 2021). Given this, to model winter flows, winter precipitation of the previous  
160 year is added as a predictor as follows:

$$161 \quad Q_{summer}(t) = a_0 + a_1 P_{winter}(t) \quad (2)$$



162 
$$Q_{winter}(t) = b_0 + b_1 P_{winter}(t) + b_2 P_{winter}(t - 1) \quad (3)$$

163 The coefficients in Eq. 2 and 3 were obtained by least square errors method during the training period. Based on this,  
164 the human influence during an evaluation (high-influence) period is obtained as:

165 
$$\Delta Q_{human} = Q_{obs} - \widehat{Q}_{nn} \pm \varepsilon \quad (4)$$

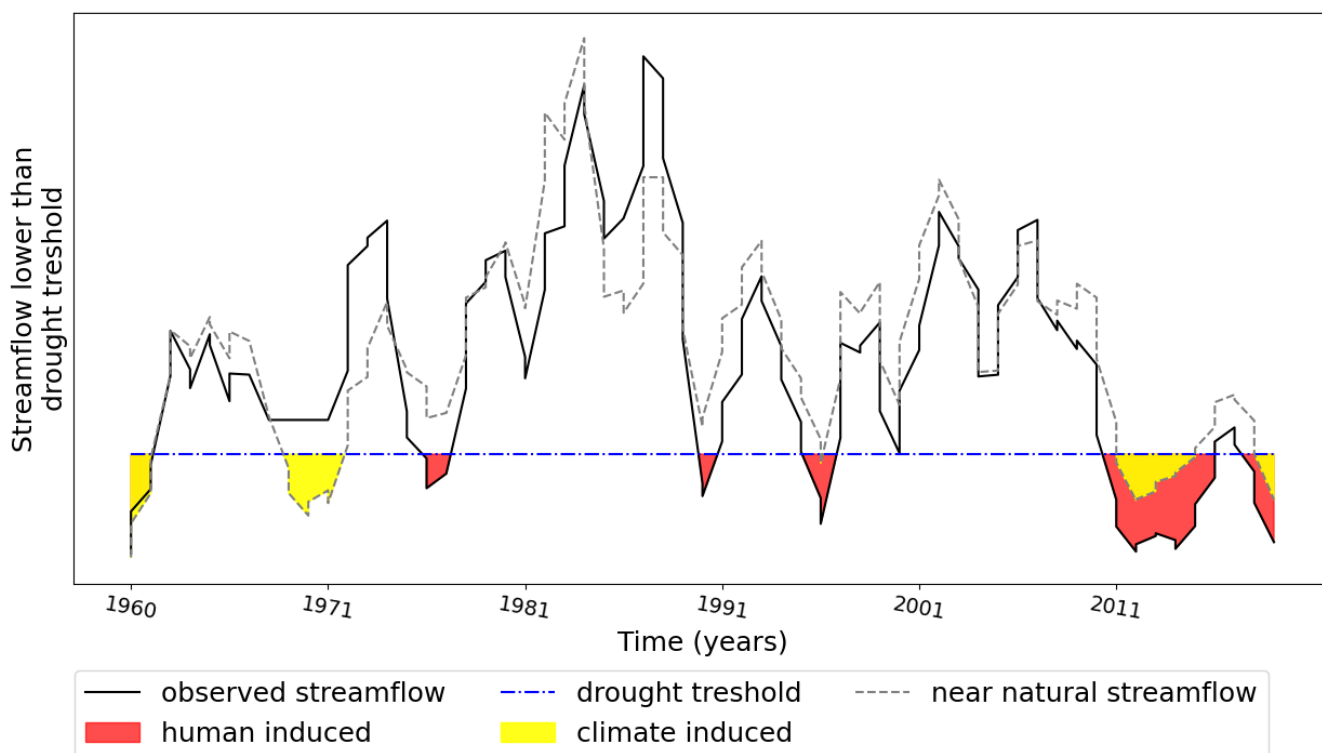
166 where  $\widehat{Q}_{nn}$  is the simulated near-natural streamflow (Eq. 2 and 3) and  $\varepsilon$  represents the uncertainty of the regression model.  
167 The attribution exercises were performed by applying Eq. 4 during the evaluation period. Noteworthy that multiple regression  
168 equations with different functional forms and variables -including evapotranspiration and temperature- were tested for  
169 representing near-natural streamflow during the reference period. The linear rainfall-runoff regressions from equations (2) and  
170 (3) were those with a higher  $r^2$ , and all variables statistically significant at a p-value of 0.05.

171 It should be noted that the near-natural streamflow estimations from Eq. 2 and 3 assume a stationary rainfall-runoff  
172 relationship. However, recent evidence has shown that, under protracted drought conditions, there is a non-stationary  
173 catchment response modulated by catchment memory that causes larger streamflow reductions to those expected from single-  
174 year precipitation deficits before the megadrought (Alvarez-Garreton et al., 2021). This evidence corresponds to the headwater  
175 near-natural basins located upstream of the human influenced basins selected in this study. To assess whether our analyses  
176 over the complete basins are potentially biased by non-stationary catchment responses, we compare the rainfall-runoff ratios  
177 (mean annual runoff normalised by mean annual precipitation) during the evaluation period before (1988-2010) and after the  
178 megadrought onset (2010-2020), in both the upper and lower sections of each basin, defined by the streamflow gauges  
179 highlighted in orange circles and red diamonds in Fig. 1, respectively.

## 180 **2.4 Hydrological drought characterisation**

181 To quantify the impact of human activities on hydrological droughts, we compared the characteristics of the observed and the  
182 near-natural streamflow deficits during drought events, including their frequency (number of drought events), duration  
183 (average, maximum and total), and intensity (i.e., deficit of volume) across the evaluation period. In this way, we can assess  
184 the relative influence of climate and human activities on the observed streamflow deficits, as schematised in Fig. 3.







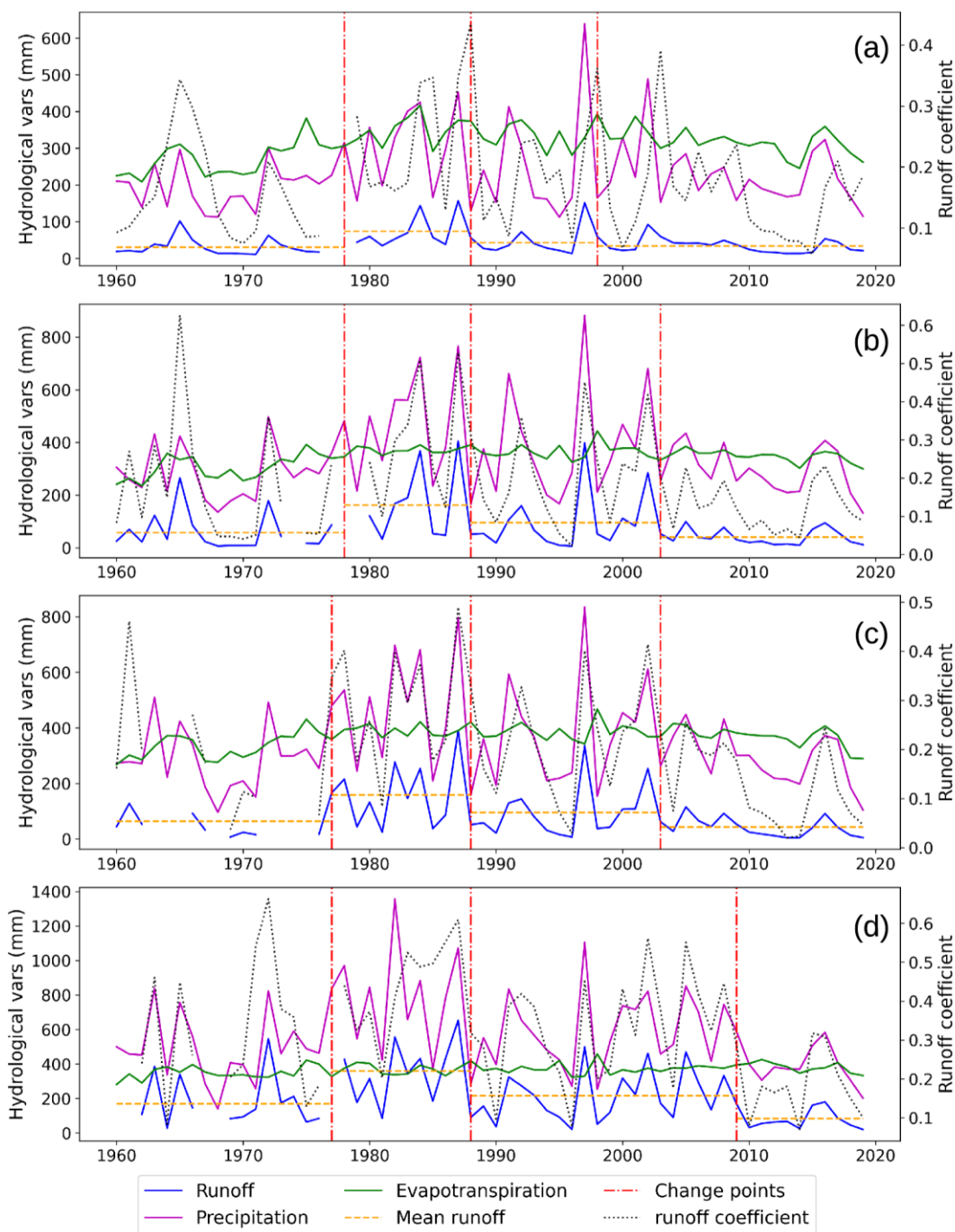
200 considering a naturalised regime. To this end, we used the observed streamflow during the training period and the near-natural  
201 simulated streamflow during the evaluation period to establish the 80th percentile of the seasonal threshold.

## 202 **3 Results**

### 203 **3.1 Low-influence periods**

204 The series of annual streamflow, precipitation, total evapotranspiration (ET), and runoff coefficients (runoff normalised by  
205 precipitation) are shown in Fig. 4. The Buishand test resulted in significant change points only in streamflow and ET. Three  
206 change points were detected in all basins, the first between the years 1977-1978, the second one in 1988, and the last one  
207 between years 1998-2010 years for the streamflow in all basins (Fig. 4), while a single change point was detected in 1973-  
208 1975 for ET in all basins except Aconcagua. The Rodionov STARS test detected similar three change points in streamflow in  
209 1977 -1981, 1988, and 2010, with the 1988 breakpoint presenting the higher R-shift index value.

210 In order to select periods with minimal human activities, it is important to identify breakpoints in the streamflow time series  
211 that are not primarily explained by climate shifts. The streamflow breakpoint of 1977-1978 is disregarded since it is mainly  
212 due to climate drivers, as indicated by the single ET breakpoint during that period. We can relate this to the great Pacific shift  
213 and the warm cycle of the Pacific Decadal Oscillation (PDO) between 1977 and the mid-1990s (Kayano et al., 2009; Jacques-  
214 Coper and Garreaud, 2015; González-Reyes et al., 2017). Additionally, the 2010 Aconcagua streamflow breakpoint is likely  
215 driven by the onset of the megadrought, which also affected the 2004 change points in the Limarí and Choapa Basins where  
216 lower precipitation was observed even before the megadrought.



217  
 218  
 219  
 220

**Figure 4. Annual streamflow, precipitation, evapotranspiration, and runoff coefficient during the complete period (1960-2020) for Elqui (a), Limarí (b), Choapa (c), and Aconcagua (d) Basins, respectively. The vertical red line indicates the years where significant change points (P value < 0.05) on streamflow distribution are detected by the Buishand test.**



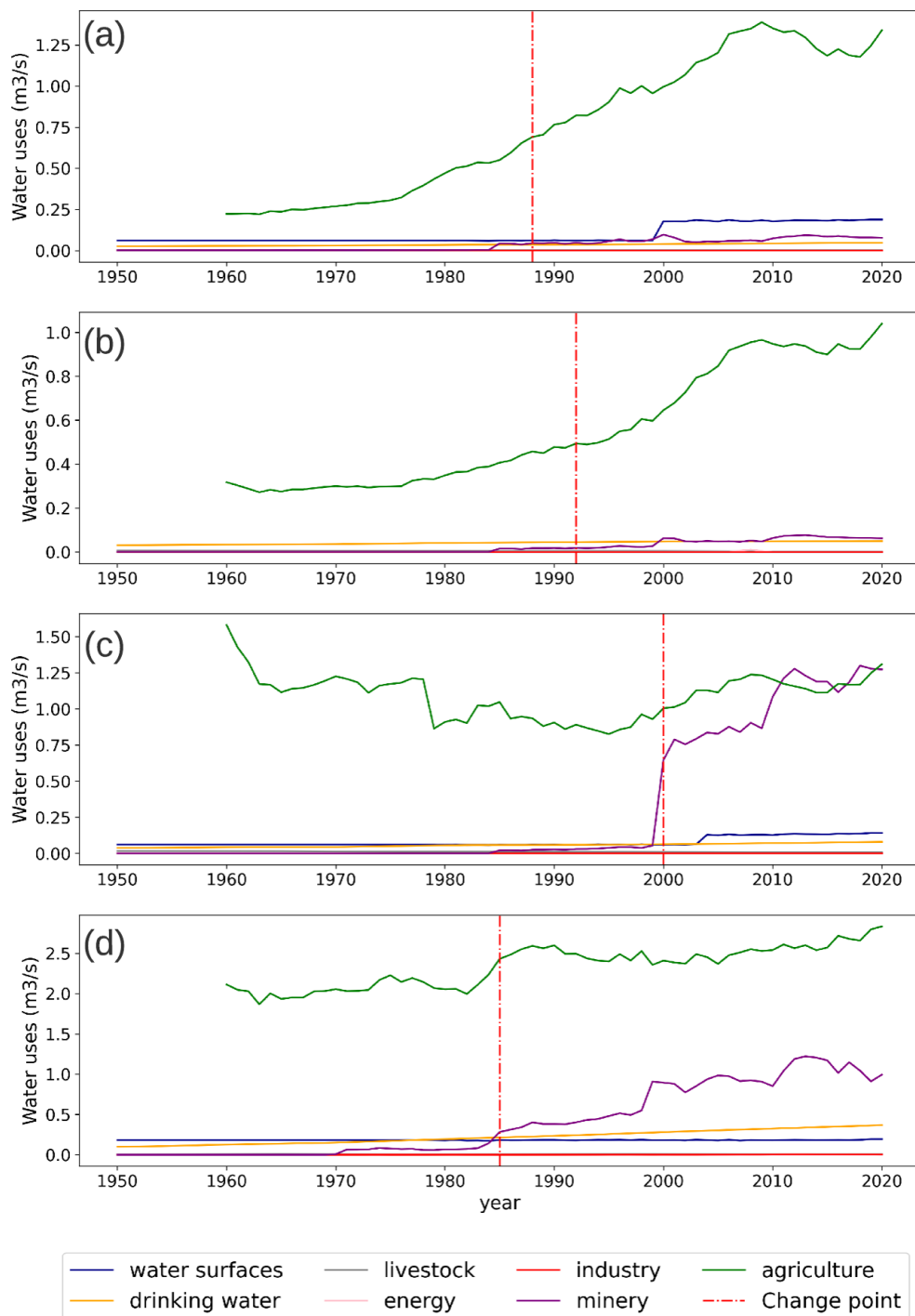
221 Regarding water use, breakpoints were observed in Elqui and Limarí in 1988 and 1992, respectively, mainly associated to the  
 222 growth of the agricultural sector (Fig. 5). In the Aconcagua basin, a breakpoint occurred in 1985 due to intensified water use  
 223 by the mining and agriculture sectors. Meanwhile, in the Choapa basin, a significant increase in mining water consumption  
 224 since 2000 explains the time series breakpoint observed in that year. The 1998 Elqui Basin streamflow breakpoint may be  
 225 attributed to the construction of a dam upstream from the gauge station considered in this study (Fig. 5). Based on these results,  
 226 we used the 1988 streamflow breakpoint observed in all basins to define the low-influence period of 1960-1988. In  
 227 consequence, the evaluation period was defined between 1988 and 2020, characterised by greater anthropogenic intervention  
 228 and by the megadrought in its second half.

229 By comparing the hydroclimatic conditions of the study basins during the low-influence and evaluation periods, we see that  
 230 the mean annual precipitation declined between 0 to 18% during these periods (Table 1). In contrast, the mean annual  
 231 streamflow decreased by a range of 14 to 35%. If we examine summer streamflow, when agricultural water consumption is  
 232 more intense, a reduction of 24 to 46% is observed. While the Aconcagua basin features the largest decrease in precipitation,  
 233 the Choapa basin has the largest decrease in streamflow.

Basin	Mean annual precipitation (mm)			Mean annual runoff (mm)			Mean summer runoff (mm)		
	Low- influence period	Evaluati on period	Difference	Low- influence period	Evaluati on period	Differenc e %	Low- influence period	Evaluati on period	Difference %
<b>Elqui</b>	232.83	232.73	0.0%	45.53	39,17	-15.9%	28.66	21.71	-24.3%
<b>Limarí</b>	355.13	336.78	-5.2%	95.91	66,92	-30.2%	54.50	33.87	-37.9%
<b>Choapa</b>	371.16	327.76	-11.7%	106.41	66,77	-37.2%	68.09	36.70	-46.1%
<b>Aconcagua</b>	634.61	533.76	-16%	258.42	173,87	-32.7%	193.29	119.82	-38.0%

234 **Table 1: Average annual precipitation, average annual streamflow, and average summer season streamflow for each basin in the**  
 235 **low-influence (1960-1988) and evaluation periods (1988-2020).**

236



237  
 238 **Figure 5.** Time series of water uses from different human activities in Elqui (a), Limarí (b), Choapa (c), and Aconcagua (d) basins,  
 239 respectively. These time series include water uses for industrial, agriculture, mining, energy, animals, water surfaces, and drinking  
 240 water sectors. The red line indicates a breakpoint in the total water use distribution.



241 **3.2 Near-natural streamflow estimation**

242 Near-natural simulated streamflow during the low-influence and evaluation periods for each basin is presented in Fig. 6. The  
 243 summer season estimations obtained from Eq. 2 had good performances during the training period, with mean biases of 0 to  
 244 5% and  $r^2$  ranging from 0.8 to 0.89 for the different basins. The winter season models resulted in lower performance, with  
 245 mean biases of 0 to 0.63% and  $r^2$  ranging from 0.61 and 0.93 among the study basins (Table 2).

Basin	Season	$r^2$	Mean bias
Elqui	Summer	0.81	-0.01%
	Winter	0.69	0%
Limari	Summer	0.84	-5%
	Winter	0.86	0.63%
Choapa	Summer	0.89	-0.05%
	Winter	0.93	0.06%
Aconcagua	Summer	0.81	0%
	Winter	0.61	0%

246 **Table 2: Seasonal model results in the calibration period.**

247 To test the potential biases induced by non-stationary catchment response during the megadrought, Table 3 shows the rainfall-  
 248 runoff ratios during the evaluation period before (1988-2010) and after the megadrought onset (2010-2020), in the upper and  
 249 lower sections of each basin, respectively. These results indicate that the mean rainfall-runoff ratios declined across all sections  
 250 and basins during the megadrought, however, the reduction in the upper sections, mostly attributed to endogenous runoff  
 251 mechanisms and hydrological memory, is less significant than that those observed downstream. Specifically, the changes in  
 252 downstream rainfall-runoff ratios are nearly four times greater than the upper stream changes in the Aconcagua and Elqui  
 253 basins, more than twice as much in Choapa, and 1.6 times greater at the Limarí station, which is the sub-basin with the lowest  
 254 level of human activity in our attribution exercise. This indicates that while endogenous runoff mechanisms, such as  
 255 hydrological memory, may contribute to larger streamflow deficits during prolonged drought in near-natural basins, human  
 256 activities in the downstream basins are inducing a larger impact in runoff generation during the megadrought.

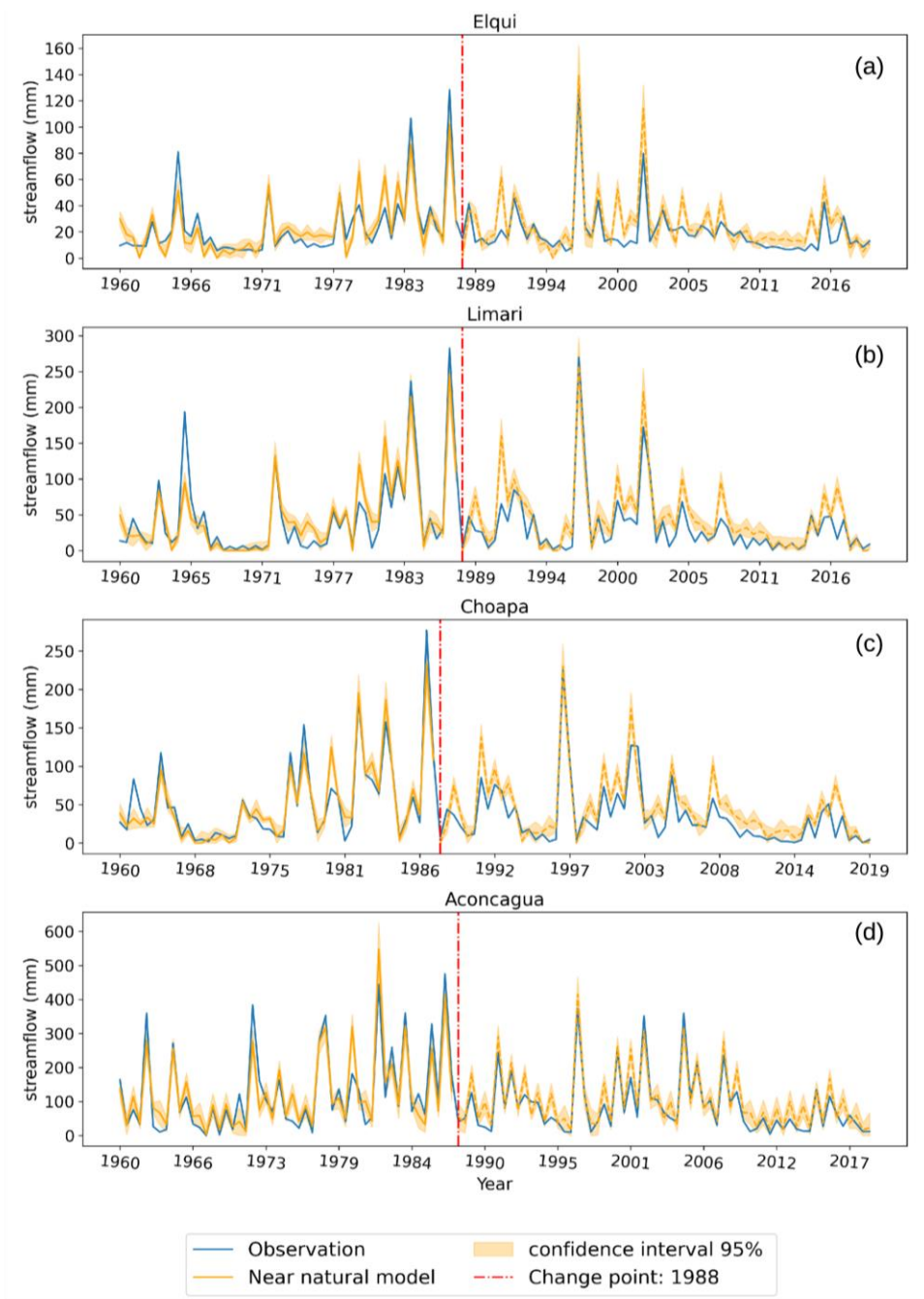
Period	Basin	Elqui		Limarí		Choapa		Aconcagua	
	Section	Upper	Lower	Upper	Lower	Upper	Lower	Upper	Lower
1988 -2010		0.42	0.19	0.41	0.18	0.58	0.21	0.75	0.33
2010 -2020		0.38	0.12	0.31	0.11	0.43	0.09	0.66	0.18
	Difference	9.03%	34.3%	25.2%	40.4%	24.94%	58.33%	11.94%	46.21%

257 **Table 3: Average annual runoff coefficient during the change period without major climate events (1988-2010) and during the**  
 258 **megadrought (2010-2020) for the upper and lower sections of each basin. The difference between the two periods relative to 1988-**  
 259 **2010 is shown in the third row.**



260 **3.3 The impacts of climate and human activities on streamflow**

261 During the evaluation period, the near-natural streamflow is higher than the observed streamflow in all the cases (Fig. 6) with  
262 mean biases in annual simulated streamflow ranging from 65% in the Limarí basin (simulated annual runoff of 55 mm and  
263 observed annual runoff of 36,7 mm) to 30% in the Aconcagua basin (simulated annual runoff of 155,4 mm and observed  
264 annual runoff of 119,8 mm).



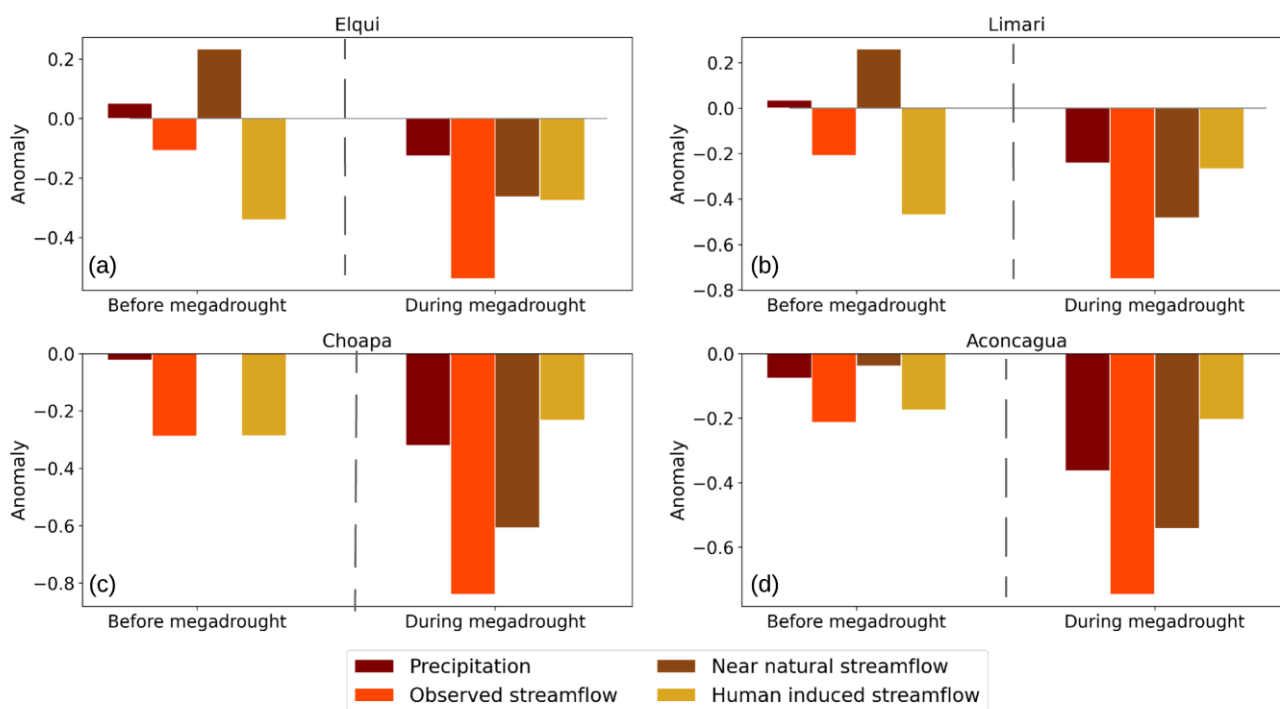
265

266 **Figure 6. The observed and near natural simulated seasonal streamflow for Elqui (a), Limarí (b), Choapa (c), and Aconcagua (d)**  
267 **basins, respectively. The continuous yellow line represents the simulated streamflow on the reference period whose  $r^2$  is presented**  
268 **on the legend. The dashed yellow line is the simulated streamflows on the change period after the breakpoint (red line). the yellow**  
269 **ban represents the 95% confidence interval.**





270 The relative impacts of climate and human activities on summer streamflow reductions during the evaluation period is  
271 presented in Fig. 7. This figure shows the annual anomalies of precipitation, observed and near-natural simulated streamflow,  
272 as well as the human-induced streamflow reduction obtained as the difference of the latter two (Eq. 4). The results for the  
273 annual fluxes are presented in Appendix A (Fig. A1).



274

275 **Figure 7: Anomalies in annual precipitation, observed summer streamflow and simulated near-natural summer streamflow, with**  
276 **the derived human-induced streamflow change for Elqui (a), Limarí (b), Choapa (c), and Aconcagua (d) basins. The anomalies are**  
277 **presented for the evaluation period before and after the megadrought onset (1988-2009 and 2010-2020, respectively). For each flux,**  
278 **the anomalies are computed as the percentage difference with respect to their mean values during the reference period (1960-1988).**

279 Before the megadrought onset, annual precipitation varied between 5 to -7.6% with respect to the 1960-1988 reference period  
280 among the study basins. The resulting near-natural summer streamflow during that period followed the direction of the annual  
281 precipitation anomalies, with anomalies between 23 to -4% across basins. During that period, the observed summer streamflow  
282 accounting for full climatic and human influences decreased by 10-28%. This indicates that water uses for human activities  
283 were the driver factor of summer streamflow reduction before the megadrought onset, causing up to 100% of reduction in  
284 Elqui, Limarí and Choapa, and 82% in the Aconcagua Basin, respectively. The human-induced decrease on Aconcagua  
285 accounts for 33.8 mm over the total streamflow deficit of 41.3 mm.



286 After the megadrought onset, the relative impact of precipitation deficits and human activities on streamflow depletion  
287 changed. The annual precipitation anomalies during the megadrought varied between -13 to -36% across basins, while the near  
288 natural streamflow estimates present anomalies between -26% to -61% with respect to the 1960-1988 reference period. During  
289 that period, the observed summer streamflow accounting for full climatic and human influences featured anomalies of -54%  
290 to -84%. This indicate that precipitation deficits dominate the streamflow reduction, however, there is still a relevant reduction  
291 of 7.9 mm, 11.9 mm, 15.5mm, and 39.5 mm attributed to human activities, representing 51%, 29%, 27%, and 27% of the total  
292 summer streamflow reduction in Elqui, Limarí, Choapa, and Aconcagua Basin, respectively.

293 Particularly noteworthy is the Aconcagua basin case, where the human induced total streamflow reduction during the  
294 megadrought (39.5 mm) is higher than in the period before the megadrought (33.8 mm) despite considerably less water  
295 availability (near natural summer streamflow estimates of 88.6 mm during the megadrought and 185,7 mm before the  
296 megadrought).

297 Consistently with the summer seasons, near-natural annual streamflow before the megadrought followed precipitation patterns,  
298 with anomalies between 22 to -5% across basins (Fig. A1). During that period, the observed annual streamflow varied between  
299 -2 to -20% across basins. Water uses for human activities were the driver factor of streamflow reduction before the  
300 megadrought onset, causing up to 100% of reduction in Elqui, Limarí and Choapa, and 71% in the Aconcagua Basin,  
301 respectively. After the megadrought onset, the observed streamflow featured anomalies of -47 to -71%. From these streamflow  
302 deficits a 44% to 75 % of the reduction is attributed to climatic-factors (i.e., anomalies represented by the near-natural  
303 simulated streamflow), while the remaining 25 to 56% is attributed to human activities.

### 304 **3.4 The impacts of human activities on hydrological drought events**

305 The hydrological drought events selected based on a seasonal threshold of 80th percentile of the near-natural streamflow (Sect.  
306 2.4) are shown in Fig. 8. By contrasting the observed and near-natural time series, the climate-induced and human-induced  
307 droughts are distinguished. The meteorological megadrought (2010-2020) is identified as a series of hydrological drought  
308 events in the observed streamflow. In contrast, it does not seem as persistent and intense in the near-natural streamflow  
309 scenario.

310 The largest human impact on hydrological droughts is observed in the total seasons in drought and the total deficit (Table 4).  
311 Elqui, Choapa, and Aconcagua have 13, 8, and 10 extra seasons of drought, respectively, and more than double (triple in  
312 Choapa's case) deficit concerning the near natural scenario. Additionally, more drought events with a larger average time  
313 duration and average deficit have occurred in the observed scenario on the three basins previously mentioned. The largest  
314 drought event in each basin occurred during the megadrought. Across all basins, the human activities led to an increase in the  
315 maximum duration of hydrological droughts, with maximum values ranging between 4 to 10 seasons, in contrast to 1 to 4

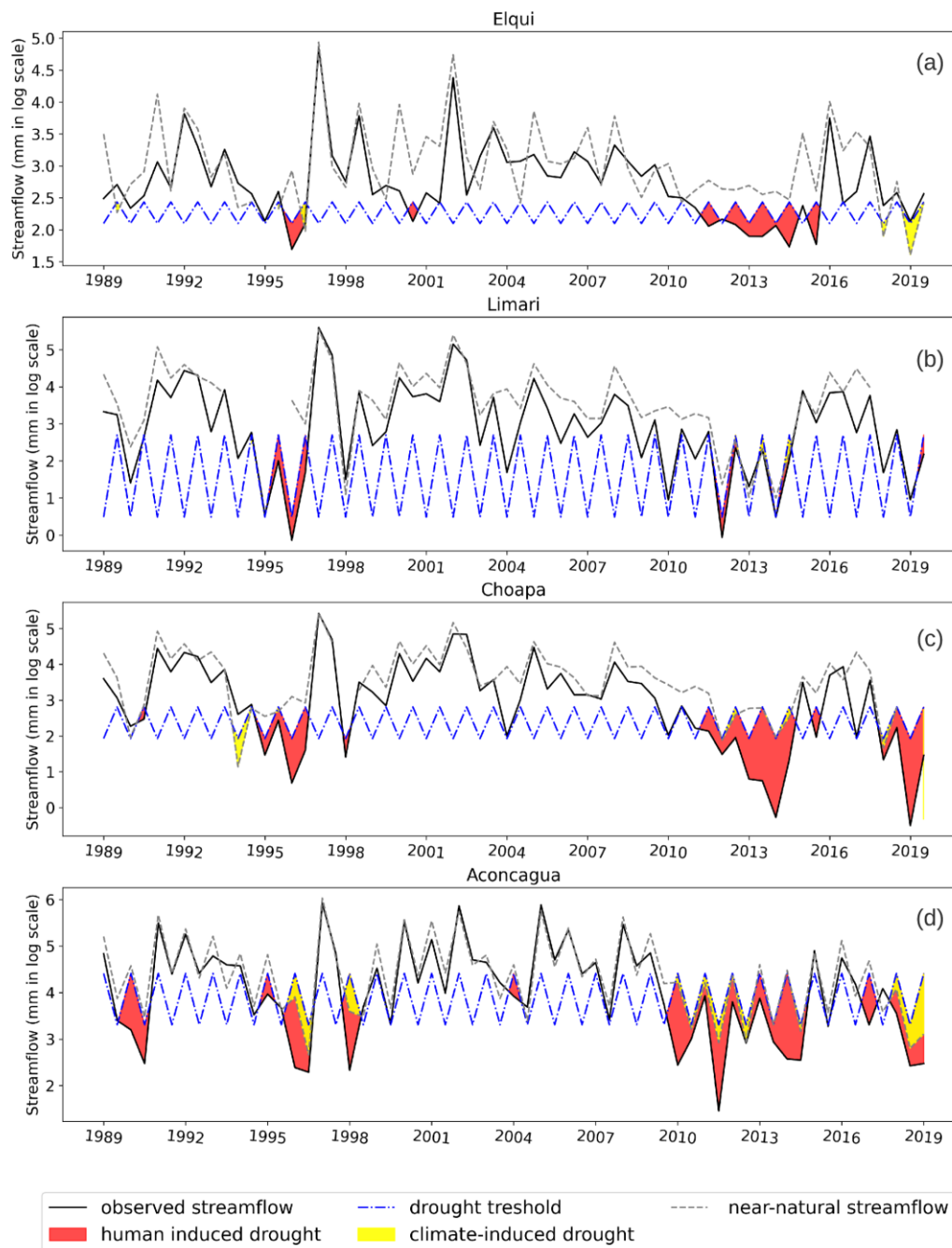


316 seasons experienced in the near-natural cases. In particular, this translates to five years of continuous streamflow below the  
 317 Q80 threshold on the Aconcagua basin.

Basin	Hydrological Droughts	frequency	duration (seasons)			deficit (mm)		
			Total season	Max duration	Average duration	Total deficit	Max deficit	Average deficit
Elqui	Near natural	5.0	5.0	1.0	1.0	21.1	10.5	4.2
	Observed	9.0	18.0	9.0	2.0	56.1	29.8	6.2
Limarí	Near natural	3.0	9.0	4.0	3.0	41.4	20.9	13.8
	Observed	6.0	13.0	4.0	2.2	47.5	20.4	7.9
Choapa	Near natural	5.0	10.0	4.0	2.0	36.1	19.6	7.2
	Observed	6.0	18.0	7.0	3.0	110.1	51.0	18.3
Aconcagua	Near natural	6.0	14.0	4.0	2.3	337.1	134.5	56.2
	Observed	10.0	24.0	10.0	2.4	732.0	276.7	73.2

318 **Table 4: drought characteristics for each basin considering the observed and simulated near natural streamflow during the**  
 319 **evaluation period (1988-2020).**

320



321

322 **Figure 8. Observed and near-natural streamflow and hydrological drought events during the evaluation period (1988–2020) for**  
323 **Elqui (a), Limari (b), Choapa (c), and Aconcagua (d) basins, respectively.**



324

## 325 **4 Discussion**

### 326 **4.1 Impact of increased human activities on water availability**

327 During the megadrought, precipitation deficits have played a more significant role on the decrease in streamflow than  
328 anthropogenic factors, however, human activities still account for approximately 27 to 29% of the streamflow reduction in the  
329 Aconcagua, Choapa, and Limarí basins and 51% in Elqui, the basin least affected by the meteorological megadrought.

330 Human activities have intensified since the 1980s and 1990s, driven by rising water demand from economic activities,  
331 population growth, and land use changes (Fig. 5a), despite the precipitation deficits and streamflow reduction during the  
332 megadrought. This suggest that total water consumption has been inelastic to the surface water deficits. In the Aconcagua  
333 basin, the total water consumption increased during the megadrought, while in the other three basins, the human-induced  
334 streamflow reduction expressed as mm is slightly smaller during the megadrought, compared to the period prior to the  
335 megadrought (Fig. 7). This finding could be explained by an initial reduction in agricultural water consumption during the first  
336 years of the megadrought, which was later reversed (Fig. 5a) by higher extractions of groundwater sources in the subsequent  
337 years (Taucare et al., 2020; Duran-Llacer et al., 2020).

338 Human activities account for approximately 25% of the reduction in streamflow during the evaluation period in most basins,  
339 and their effects on hydrological droughts have been significant. Despite experiencing lower precipitation deficits, the Elqui  
340 basin shows a similar pattern of hydrological drought recurrence, total seasons, and maximum duration compared to the Choapa  
341 and Aconcagua basins. During the megadrought, this basin was the most affected by increased human activities, with the  
342 number of drought seasons increasing from 5 in the near natural scenario to 18 in the observed data. This suggests that increased  
343 and inelastic human water demands are particularly relevant in semi-arid basins with limited precipitation and high interannual  
344 variability in terms of precipitation regime, such as Elqui, making them more prone to experience a more severe hydrological  
345 drought during precipitation deficits. This is consistent with Huang (2016), who highlighted that sustainable agricultural  
346 development is threatened in arid and semi-arid regions due to limited available water resources, and with Saft et al. (2016),  
347 who demonstrated that aridity is a crucial factor influencing sensitivity to interdecadal climate variability.

### 348 **4.2 Drought vulnerability**

349 Hydrological drought vulnerability is associated with those conditions that cause an increase in the frequency, duration, and  
350 intensity of the hydrological droughts when a precipitation deficit threat is faced. Vulnerability should be addressed by looking  
351 for sensitivity variables that come from the biophysical basin's characteristics, such as aridity, location, geomorphology,



352 hydrological regime, natural land cover, and snow and glacier cover (Saft et al., 2015; Van Loon and Laaha, 2015), and human  
353 activities such as management and extraction of water, land use, land cover changes, urbanisation, between others (Barría et  
354 al., 2021a; Van Loon et al., 2016, 2022). Although several articles have assessed hydrological drought vulnerability by  
355 evaluating biophysical basin characteristics (Alvarez-Garreton et al., 2021; Van Loon and Laaha, 2015; Saft et al., 2015; Van  
356 Lanen et al., 2013), there is still a gap in understanding how human activities contribute to basin's vulnerability to drought.

357 As discussed in Sect. 4.1, human activities have intensified streamflow deficits during the megadrought. Although our results  
358 correspond to four basins in central Chile, the large streamflow deficits have been reported over a wider region, with a range  
359 of impacts on society and ecosystems. For example, (Miranda et al., 2020) reported that watercourses stopped flowing at  
360 certain periods of the year during the megadrought, while a significant effect has been observed on forest productivity with  
361 high tree mortality. Additionally, thousands of people have lost access to domestic water services (Muñoz et al., 2020).  
362 National statistics indicate that spending on cistern trucks to deliver potable water to rural communities in the six main  
363 watersheds of Coquimbo and Valparaíso regions reached US\$56 million during 2010-2020. Human activities that affect  
364 catchment vulnerability in central Chile include groundwater extractions (Taucare et al., 2020), overallocation of water use  
365 rights (Alvarez-Garreton et al., 2021; Barría et al., 2021a), and continuous land use change for agricultural purposes  
366 (Madariaga et al., 2021). For example, agriculture is sometimes established on hillsides with high slopes, exacerbating water  
367 consumption problems and changing runoff mechanisms. In the entire Aconcagua basin, the water consumption of avocado  
368 plantations has increased 15% between 2014 and 2020, reaching almost 4.8 M<sup>3</sup>/s, while citrus plantations have increased 67-  
369 70% in the Elqui and Limarí basins since 2010, reaching 1.8 M<sup>3</sup>/s of water consumption in the Limarí basin. This reveals that  
370 water use for agriculture activities has been inelastic to the precipitation deficits during the megadrought. Human activities in  
371 these basins are adapting to less water availability in ways that are leading to aggravated water scarcity problems, which is  
372 consider in the literature as maladaptation (Schipper, 2020).

## 373 **5 Conclusions**

374 The megadrought in central Chile corresponds to the longest dry period over the last centuries. The study basins featured a  
375 range of 16-41% in mean annual precipitation deficits during this period, whereas the deficits in streamflow were significantly  
376 larger. The Elqui, Limarí, Choapa, and Aconcagua Basin experienced deficits in summer streamflow of 54%, 75%, 84%, and  
377 75%, respectively.

378 Our findings indicate that human activities were the main driving factor of streamflow reduction before the megadrought began  
379 in 2010. During the megadrought, human activities still accounted for a significant portion of streamflow reduction, ranging  
380 from 27 to 51%. The impact of human activities on hydrological drought characteristics was substantial, leading to more than



381 double the recurrence, duration, and intensity of droughts in some basins. Furthermore, our results show that human activities  
382 have dominated the decline of the rainfall-runoff ratios during the megadrought in the study basins.

383 Human activities in these basins show limited adaptation to the decreasing water availability. During the megadrought, new  
384 surface and underground water use rights have been granted (Barría et al., 2021b). The increase in human water demand, often  
385 inelastic to the decreased surface water availability, makes basins more vulnerable to severe hydrological droughts when  
386 precipitation deficits are faced, especially on semi-arid basins with water availability constraints.

387 This paper demonstrates that during long and persistent dry periods, human activities within the catchment strongly influence  
388 the intensity and duration of hydrological drought. To effectively adapt to climate change and avoid maladaptation measures,  
389 it is necessary to consider the feedback between water use, anthropogenic activity, and the hydrological system. These  
390 considerations are particularly important in Chile and other territories around the world, where the dry signal is consistent and  
391 expected to persist.

#### 392 **Data availability**

393 The CR2MET dataset were obtained from the Center for Climate and Resilience Research website at [https://www.cr2.cl/datos-](https://www.cr2.cl/datos-productos-grillados)  
394 [productos-grillados](https://www.cr2.cl/datos-productos-grillados) (last access: 20 September 2023). The water use data was obtained upon request from the Center for  
395 Climate and Resilience Research website at <https://seguridadhidrica.cr2.cl> (last access: 20 September 2023). The streamflow  
396 data were obtained from CAMELS-CL dataset (Alvarez-Garreton et al., 2018), available at the Center for Climate and  
397 Resilience Research website at <https://camels.cr2.cl> (last access: 20 September 2023).

#### 398 **Author contributions**

399 NA, CAG and AM conceived the idea of the research. NA performed the analyses. NA and CAG wrote much of the manuscript.  
400 All the authors reviewed early manuscript drafts and the final draft.

#### 401 **Competing interests**

402 The contact author has declared that none of the authors has any competing interests.



403 **Acknowledgements:**

404 This research has been developed within the framework of the Center for Climate and Resilience Research (CR2,  
405 ANID/FONDAP/1522A0001), the research project ANID/FSEQ210001 and ANID/FONDECYT/1201714

406 **References**

- 407 Alvarez-Garreton, C., Mendoza, P. A., Pablo Boisier, J., Addor, N., Galleguillos, M., Zambrano-Bigiarini, M., Lara, A.,  
408 Puelma, C., Cortes, G., Garreaud, R., McPhee, J., and Ayala, A.: The CAMELS-CL dataset: Catchment attributes and  
409 meteorology for large sample studies-Chile dataset, *Hydrol. Earth Syst. Sci.*, 22, 5817–5846, [https://doi.org/10.5194/hess-](https://doi.org/10.5194/hess-22-5817-2018)  
410 22-5817-2018, 2018.
- 411 Alvarez-Garreton, C., Pablo Boisier, J., Garreaud, R., Seibert, J., and Vis, M.: Progressive water deficits during multiyear  
412 droughts in basins with long hydrological memory in Chile, *Hydrol. Earth Syst. Sci.*, 25, 429–446,  
413 <https://doi.org/10.5194/hess-25-429-2021>, 2021.
- 414 Barría, P., Sandoval, I. B., Guzman, C., Chadwick, C., Alvarez-Garreton, C., Díaz-Vasconcellos, R., Ocampo-Melgar, A., and  
415 Fuster, R.: Water allocation under climate change: A diagnosis of the Chilean system, *Elementa*, 9, 1–20,  
416 <https://doi.org/10.1525/elementa.2020.00131>, 2021a.
- 417 Barría, P., Chadwick, C., Ocampo-Melgar, A., Galleguillos, M., Garreaud, R., Díaz-Vasconcellos, R., Poblete, D., Rubio-  
418 Álvarez, E., and Poblete-Caballero, D.: Water management or megadrought: what caused the Chilean Aculeo Lake drying?,  
419 <https://doi.org/10.1007/s10113-021-01750-w>, 2021b.
- 420 CR2MET: A high-resolution precipitation and temperature dataset for the period 1960-2021 in continental Chile:  
421 <https://doi.org/10.5281/zenodo.7529682>, last access: 10 December 2022.
- 422 Boisier, J. P., Alvarez-Garreton, C., Cordero, R. R., Damiani, A., Gallardo, L., Garreaud, R. D., Lambert, F., Ramallo, C.,  
423 Rojas, M., and Rondanelli, R.: Anthropogenic drying in central-southern Chile evidenced by long-term observations and  
424 climate model simulations, *Elementa*, 6, 74, <https://doi.org/10.1525/elementa.328>, 2018.
- 425 Bozkurt, D., Rojas, M., Boisier, J. P., and Valdivieso, J.: Climate change impacts on hydroclimatic regimes and extremes over  
426 Andean basins in central Chile, *Hydrol. Earth Syst. Sci. Discuss.*, 17, 1–29, <https://doi.org/10.5194/hess-2016-690>, 2017.
- 427 Budds, J.: La demanda, evaluación y asignación del agua en el contexto de escasez, *Rev. Geogr. Norte Gd.*, 52, 167–184, 2012.
- 428 Buishand, T. A.: Some methods for testing the homogeneity of rainfall records, *J. Hydrol.*, 58, 11–27,  
429 [https://doi.org/10.1016/0022-1694\(82\)90066-X](https://doi.org/10.1016/0022-1694(82)90066-X), 1982.
- 430 Crespo, S. A., Lavergne, C., Fernandoy, F., Muñoz, A. A., Cara, L., and Olfos-Vargas, S.: Where does the Chilean Aconcagua  
431 river come from? Use of natural tracers for water genesis characterization in glacial and periglacial environments, *Water*  
432 (Switzerland), 12, <https://doi.org/10.3390/w12092630>, 2020.
- 433 Duran-Llacer, I., Munizaga, J., Arumí, J. L., Ruybal, C., Aguayo, M., Sáez-Carrillo, K., Arriagada, L., and Rojas, O.: Lessons





- 434 to be learned: Groundwater depletion in Chile's ligua and petorca watersheds through an interdisciplinary approach, *Water*  
435 (Switzerland), 12, <https://doi.org/10.3390/w12092446>, 2020.
- 436 Esri. "Topographic" [basemap]. Scale Not Given. "World Topographic Map". 2017.  
437 <https://www.arcgis.com/home/item.html?id=7dc6cea0b1764a1f9af2e679f642f0f5>. (October 24, 2023).
- 438 Fleig, A. K., Tallaksen, L. M., Hisdal, H., Stahl, K., and Hannah, D. M.: Inter-comparison of weather and circulation type  
439 classifications for hydrological drought development, *Phys. Chem. Earth*, 35, 507–515,  
440 <https://doi.org/10.1016/j.pce.2009.11.005>, 2010.
- 441 Garreaud, R., Alvarez-Garretón, C., Barichivich, J., Pablo Boisier, J., Christie, D., Galleguillos, M., LeQuesne, C., McPhee,  
442 J., and Zambrano-Bigiarini, M.: The 2010–2015 megadrought in central Chile: Impacts on regional hydroclimate and  
443 vegetation, *Hydrol. Earth Syst. Sci.*, 21, 6307–6327, <https://doi.org/10.5194/hess-21-6307-2017>, 2017.
- 444 Garreaud, R., Boisier, J. P., Rondanelli, R., Montecinos, A., Sepúlveda, H. H., and Veloso-Aguila, D.: The Central Chile Mega  
445 Drought (2010–2018): A climate dynamics perspective, *Int. J. Climatol.*, 40, 421–439, <https://doi.org/10.1002/joc.6219>,  
446 2020.
- 447 González-Reyes, Á., McPhee, J., Christie, D. A., Quesne, C. Le, Szejner, P., Masiokas, M. H., Villalba, R., Muñoz, A. A., and  
448 Crespo, S.: Spatiotemporal variations in hydroclimate across the Mediterranean Andes (30°–37°S) since the early twentieth  
449 century, *J. Hydrometeorol.*, 18, 1929–1942, <https://doi.org/10.1175/JHM-D-16-0004.1>, 2017.
- 450 González-Reyes, Á., Jacques-Coper, M., Bravo, C., Rojas, M., and Garreaud, R.: Evolution of heatwaves in Chile since 1980,  
451 *Weather Clim. Extrem.*, 41, 100588, <https://doi.org/10.1016/j.wace.2023.100588>, 2023.
- 452 Huang, S., Liu, D., Huang, Q., and Chen, Y.: Contributions of climate variability and human activities to the variation of runoff  
453 in the Wei River Basin, China, *Hydrol. Sci. J.*, 61, 1026–1039, <https://doi.org/10.1080/02626667.2014.959955>, 2016.
- 454 Jacques-Coper, M. and Garreaud, R. D.: Characterization of the 1970s climate shift in South America, *Int. J. Climatol.*, 35,  
455 2164–2179, <https://doi.org/10.1002/joc.4120>, 2015.
- 456 Kayano, M., de Oliveira, C., and Andreoli, R.: Interannual relations between South American rainfall and tropical sea surface  
457 temperature anomalies before and after 1976, *Int. J. Climatol.*, 29, <https://doi.org/10.1002/joc.1824>, 2009.
- 458 Kingston, D. G., Stagge, J. H., Tallaksen, L. M., and Hannah, D. M.: European-scale drought: Understanding connections  
459 between atmospheric circulation and meteorological drought indices, *J. Clim.*, 28, 505–516, <https://doi.org/10.1175/JCLI-D-14-00001.1>, 2015.
- 461 Kong, D., Miao, C., Wu, J., and Duan, Q.: Impact assessment of climate change and human activities on net runoff in the  
462 Yellow River Basin from 1951 to 2012, *Ecol. Eng.*, 91, 566–573, <https://doi.org/10.1016/j.ecoleng.2016.02.023>, 2016.
- 463 Li, J., Xie, S. P., Cook, E. R., Chen, F., Shi, J., Zhang, D. D., Fang, K., Gou, X., Li, T., Peng, J., Shi, S., and Zhao, Y.:  
464 Deciphering Human Contributions to Yellow River Flow Reductions and Downstream Drying Using Centuries-Long Tree  
465 Ring Records, *Geophys. Res. Lett.*, 46, 898–905, <https://doi.org/10.1029/2018GL081090>, 2019.
- 466 Linton, J. and Budds, J.: The hydrosocial cycle: Defining and mobilizing a relational-dialectical approach to water, *Geoforum*,



- 467 57, 170–180, <https://doi.org/10.1016/j.geoforum.2013.10.008>, 2014.
- 468 Liu, Y., Ren, L., Zhu, Y., Yang, X., Yuan, F., Jiang, S., and Ma, M.: Evolution of Hydrological Drought in Human Disturbed  
469 Areas: A Case Study in the Laohahe Catchment, Northern China, *Adv. Meteorol.*, 2016,  
470 <https://doi.org/10.1155/2016/5102568>, 2016.
- 471 Madariaga, A., Maillet, A., and Rozas, J.: Multilevel business power in environmental politics: the avocado boom and water  
472 scarcity in Chile, *Env. Polit.*, 30, 1174–1195, <https://doi.org/10.1080/09644016.2021.1892981>, 2021.
- 473 Miranda, A., Lara, A., Altamirano, A., Di Bella, C., González, M. E., and Julio Camarero, J.: Forest browning trends in  
474 response to drought in a highly threatened mediterranean landscape of South America, *Ecol. Indic.*, 115, 106401,  
475 <https://doi.org/10.1016/j.ecolind.2020.106401>, 2020.
- 476 Muñoz-Sabater, J., Dutra, E., Agustí-Panareda, A., Albergel, C., Arduini, G., Balsamo, G., Boussetta, S., Choulga, M.,  
477 Harrigan, S., Hersbach, H., Martens, B., Miralles, D. G., Piles, M., Rodríguez-Fernández, N. J., Zsoter, E., Buontempo, C.,  
478 and Thépaut, J. N.: ERA5-Land: A state-of-the-art global reanalysis dataset for land applications, *Earth Syst. Sci. Data*, 13,  
479 4349–4383, <https://doi.org/10.5194/essd-13-4349-2021>, 2021.
- 480 Muñoz, A. A., Klock-Barría, K., Alvarez-Garretón, C., Aguilera-Betti, I., González-Reyes, Á., Lastra, J. A., Chávez, R. O.,  
481 Barría, P., Christie, D., Rojas-Badilla, M., and Lequesne, C.: Water crisis in petorca basin, Chile: The combined effects of  
482 a mega-drought and water management, *Water (Switzerland)*, 12, <https://doi.org/10.3390/w12030648>, 2020.
- 483 Rangelcroft, S., Van Loon, A. F., Maureira, H., Verbist, K., and Hannah, D. M.: An observation-based method to quantify the  
484 human influence on hydrological drought: upstream–downstream comparison, *Hydrol. Sci. J.*, 64, 276–287,  
485 <https://doi.org/10.1080/02626667.2019.1581365>, 2019.
- 486 Rodionov, S. N.: A sequential algorithm for testing climate regime shifts, *Geophys. Res. Lett.*, 31, 2–5,  
487 <https://doi.org/10.1029/2004GL019448>, 2004.
- 488 Saft, M., Western, A. W., Zhang, L., Peel, M. C., and Potter, N. J.: The influence of multiyear drought on the annual rainfall-  
489 runoff relationship: An Australian perspective, *Water Resour. Res.*, 51, 2444–2463,  
490 <https://doi.org/10.1002/2014WR015348>, 2015.
- 491 Schipper, E. L. F.: Maladaptation: When Adaptation to Climate Change Goes Very Wrong, *One Earth*, 3, 409–414,  
492 <https://doi.org/10.1016/j.oneear.2020.09.014>, 2020.
- 493 Sharifi, A., Mirabbasi, R., Ali Nasr-Esfahani, M., Torabi Haghighi, A., and Fatahi Nafchi, R.: Quantify the impacts of  
494 anthropogenic changes and climate variability on runoff changes in central plateau of Iran using nine methods, *J. Hydrol.*,  
495 603, 127045, <https://doi.org/10.1016/j.jhydrol.2021.127045>, 2021.
- 496 Shourov, M. M. H.: mmhs013/pyHomogeneity: tag for Zenodo Release, <https://doi.org/10.5281/ZENODO.3785287>, 2020.
- 497 Taucare, M., Daniele, L., Viguier, B., Vallejos, A., and Arancibia, G.: Groundwater resources and recharge processes in the  
498 Western Andean Front of Central Chile, *Sci. Total Environ.*, 722, 137824, <https://doi.org/10.1016/j.scitotenv.2020.137824>,  
499 2020.

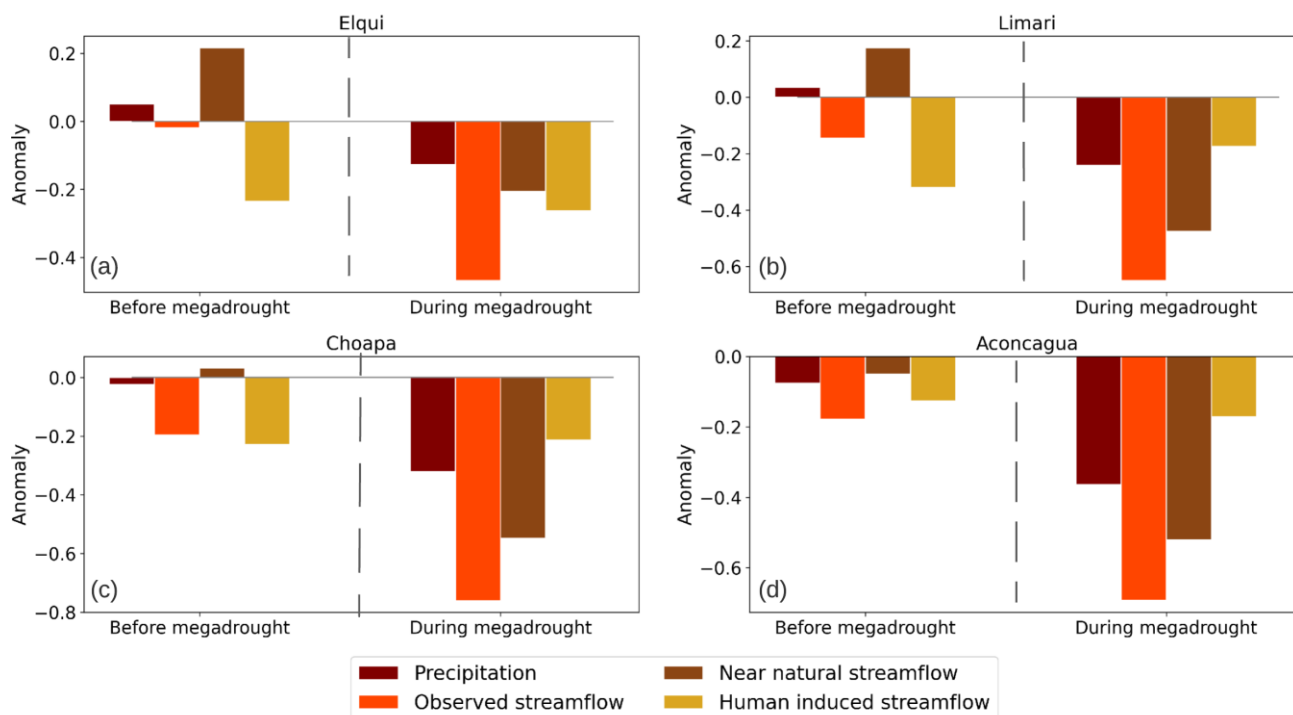


- 500 Van Lanen, H. A. J., Wanders, N., Tallaksen, L. M., and Van Loon, A. F.: Hydrological drought across the world: Impact of  
501 climate and physical catchment structure, *Hydrol. Earth Syst. Sci.*, 17, 1715–1732, [https://doi.org/10.5194/hess-17-1715-](https://doi.org/10.5194/hess-17-1715-2013)  
502 2013, 2013.
- 503 Van Loon, A. F.: Hydrological drought explained, *Wiley Interdiscip. Rev. Water*, 2, 359–392,  
504 <https://doi.org/10.1002/WAT2.1085>, 2015.
- 505 Van Loon, A. F. and Laaha, G.: Hydrological drought severity explained by climate and catchment characteristics, *J. Hydrol.*,  
506 526, 3–14, <https://doi.org/10.1016/j.jhydrol.2014.10.059>, 2015.
- 507 Van Loon, A. F., Stahl, K., Di Baldassarre, G., Clark, J., Rangelcroft, S., Wanders, N., Gleeson, T., Van Dijk, A. I. J. M.,  
508 Tallaksen, L. M., Hannaford, J., Uijlenhoet, R., Teuling, A. J., Hannah, D. M., Sheffield, J., Svoboda, M., Verbeiren, B.,  
509 Wagener, T., and Van Lanen, H. A. J.: Drought in a human-modified world: Reframing drought definitions, understanding,  
510 and analysis approaches, *Hydrol. Earth Syst. Sci.*, 20, 3631–3650, <https://doi.org/10.5194/hess-20-3631-2016>, 2016.
- 511 Van Loon, A. F., Rangelcroft, S., Coxon, G., Naranjo, J. A. B., Van Ogtrop, F., and Van Lanen, H. A. J.: Using paired  
512 catchments to quantify the human influence on hydrological droughts, *Hydrol. Earth Syst. Sci.*, 23, 1725–1739,  
513 <https://doi.org/10.5194/hess-23-1725-2019>, 2019.
- 514 Van Loon, A. F., Rangelcroft, S., Coxon, G., Werner, M., Wanders, N., Di Baldassarre, G., Tjiedeman, E., Bosman, M., Gleeson,  
515 T., Nauditt, A., Aghakouchak, A., Breña-Naranjo, J. A., Cenobio-Cruz, O., Costa, A. C., Fendekova, M., Jewitt, G.,  
516 Kingston, D. G., Loft, J., Mager, S. M., Mallakpour, I., Masih, I., Maureira-Cortés, H., Toth, E., Van Oel, P., Van Ogtrop,  
517 F., Verbist, K., Vidal, J. P., Wen, L., Yu, M., Yuan, X., Zhang, M., and Van Lanen, H. A. J.: Streamflow droughts  
518 aggravated by human activities despite management, *Environ. Res. Lett.*, 17, 044059, [https://doi.org/10.1088/1748-](https://doi.org/10.1088/1748-9326/ac5def)  
519 9326/ac5def, 2022.
- 520 Wanders, N. and Wada, Y.: Human and climate impacts on the 21st century hydrological drought, *J. Hydrol.*, 526, 208–220,  
521 <https://doi.org/10.1016/j.jhydrol.2014.10.047>, 2015.
- 522 Ward, P. J., de Ruiter, M. C., Mård, J., Schröter, K., Van Loon, A., Veldkamp, T., von Uexkull, N., Wanders, N.,  
523 AghaKouchak, A., Arnbjerg-Nielsen, K., Capewell, L., Carmen Llasat, M., Day, R., Dewals, B., Di Baldassarre, G.,  
524 Huning, L. S., Kreibich, H., Mazzoleni, M., Savelli, E., Teutschbein, C., van den Berg, H., van der Heijden, A., Vincken,  
525 J. M. R., Waterloo, M. J., and Wens, M.: The need to integrate flood and drought disaster risk reduction strategies, *Water*  
526 *Secur.*, 11, <https://doi.org/10.1016/j.wasec.2020.100070>, 2020.
- 527 Zhao, G., Tian, P., Mu, X., Jiao, J., Wang, F., and Gao, P.: Quantifying the impact of climate variability and human activities  
528 on streamflow in the middle reaches of the Yellow River basin, China, *J. Hydrol.*, 519, 387–398,  
529 <https://doi.org/10.1016/j.jhydrol.2014.07.014>, 2014.
- 530 Zhao, Y., Feng, D., Yu, L., Wang, X., Chen, Y., Bai, Y., Hernández, H. J., Galleguillos, M., Estades, C., Biging, G. S., Radke,  
531 J. D., and Gong, P.: Detailed dynamic land cover mapping of Chile: Accuracy improvement by integrating multi-temporal  
532 data, *Remote Sens. Environ.*, 183, 170–185, <https://doi.org/10.1016/j.rse.2016.05.016>, 2016.



533

534 **Appendix 1**



535

536 **Figure A1: Anomalies in annual precipitation, observed streamflow, simulated near-natural streamflow and human-induced**  
537 **streamflow change. The anomalies are presented for the evaluation period before and after the megadrought onset (1988-2009 and**  
538 **2010-2020, respectively). For each flux, the anomalies are computed as the percentage difference with respect to their mean values**  
539 **during the low-influence reference period (1960-1988). The graphs show these results for Elqui (a), Limari (b), Choapa (c), and**  
540 **Aconcagua (d) Basins, respectively**

541